Tunable plasmonic and structural properties of SnO_2: Au thin films deposited via GLAD-enhanced DC Sputtering

Rofaida Nezzar[1], Nicolas Martin[2] and Faycal Djeffal[1,*]
[1] LEA, Department of Electronics, University of Batna 2, Batna 05000, Algeria
[2] SUPMICROTECH, CNRS, Institut FEMTO-ST, BESANCON Cedex, France
*E-mail:faycal.djeffal@univ-batna2.dz

Abstract:

This study investigates the impact of deposition angle on the structural and optical properties of Au-doped SnO_2 thin films synthesized via DC sputtering combined with GLancing Angle Deposition (GLAD). Thin films were deposited at particle flux angles of 0° (planar), 40°, 60°, and 80° (oblique). X-ray diffraction (XRD) analysis confirmed the polycrystalline nature of SnO_2 and the successful incorporation of gold as a metallic nanocrystalline phase. The results revealed that GLAD significantly influences the film microstructure, altering crystallite size and preferred orientation. Optical measurements showed a progressive decrease in transparency with increasing deposition angle, with transmittance at 550 nm decreasing from 48% (planar) to 30% (80°), primarily due to enhanced light scattering from the nanostructured, porous morphology induced by GLAD. Interestingly, a slight reduction in absorbance at 550 nm was also observed in obliquely deposited films. The incorporation of gold as a dopant introduced localized surface plasmon resonance (LSPR) effects, significantly enhancing light absorption and scattering near the plasmonic peak. Notably, the LSPR peak position was tunable from approximately 550 nm to 680 nm, depending on the GLancing angle during deposition. Despite notable structural and optical changes, the optical band gap remained relatively stable, ranging from 3.88 to 3.95 eV across all samples. Overall, this work highlights the synergistic effect of GLAD and gold doping in accurately tuning the plasmonic and microstructural characteristics of SnO_2 thin films, making them promising candidates for a broad range of optoelectronic applications, including photodetectors, solar cells, and chemical or biological sensors.

Keywords: GLAD; GLancing; Tin Dioxide; Gold; Plasmonics; LSPR; DC sputtering.

1. Introduction

Thin film materials serve an essential role in a wide range of modern technologies. Optoelectronic devices [1] stand at the forefront of these innovations, driving advancements in areas such as solar cells, touchscreens, light-emitting diodes (LEDs) and smart windows [2]. The performance of these devices relies heavily on the accurate engineering of their constituent materials, particularly wide bandgap semiconductors and transparent conductive oxides (TCOs) [3-6]. These materials are capable of fine-tuning electrical and optical properties at the atomic level, effective for efficient charge transport and light manipulation [7]. Among these, tin dioxide (SnO_2) [8] has emerged as a well-known TCO, acknowledged due to its wide bandgap which enables exceptional optical transparency, high electrical conductivity and robust chemical stability [9], [10]. Despite its foundational strengths, the intrinsic properties of SnO_2 present certain performance restrictions. Its relatively low electron mobility and constrained absorption in specific spectral regions can limit its full potential in high-performance optoelectronic systems, especially those requiring strong light-matter interaction like photovoltaic cells [11-13]. To overcome these challenges, a complex, multi-faceted approach to materials engineering is required. An important tactic involves compositional modification through doping SnO_2 with noble metals like gold (Au) [14], [15] . The introduction of gold nanoparticles into the tin dioxide matrix unlocks powerful plasmonic effects, most notably Localized Surface Plasmon Resonance (LSPR), the phenomenon where the collective oscillation of electrons on the surface of the gold nanoparticles strongly couples with incident light, leading to enhanced light scattering and absorption [16], [17]. This procedure not only augments the film's light-harvesting capability but also greatly facilitates the generation of charge carriers, thereby significantly improving the overall performance of optoelectronic devices.

Dense, homogeneous layers are frequently produced by conventional thin-film deposition methods, although these may not be ideal for applications needing a large surface area or precise light control. This is where the GLancing Angle Deposition (GLAD) [18], [19] method represents a paradigm shift. Unlike conventional sputtering where particles arrive perpendicularly, GLAD directs the particle flux at a highly oblique angle which creates a geometric shadowing effect at the substrate surface, allowing for a precise control of nanoscale morphology. The manipulation of the deposition angle, GLAD facilitates the growth of unique anisotropic structures, from inclined columns and patterns to intricate porous networks [19], [20]. This structural control provides an unprecedented level of freedom in fabricating the film's surface area, porosity, and light-trapping capabilities. The true synergy of this approach lies in the combination of these two techniques. When paired with noble metal doping, GLAD not only controls the morphology of the host SnO_2 matrix but also dictates the formation and spatial distribution of the gold nanoparticles within it.

This paper presents a focused study into the structural and optical characterization of gold-doped Tin dioxide (SnO_2:Au) thin films. The films were prepared using a DC sputtering system integrated with the GLAD technique, which allowed for the systematic study of the deposition angle's influence. Specifically, this work contrasts films grown at a planar angle (α=0°) against those prepared at oblique angles (α=40°, 60°, and 80°). The main objective here is to inspect the resulting crystalline structure and optical transmittance, providing a basic grasp of how the GLAD-induced morphology, coupled with plasmonic gold doping, dictates the films' characteristics. The insights extracted from this research are critical for establishing a foundational material science framework for gold doped tin dioxide thin films. Ultimately, this work offers a clear roadmap for optimizing these advanced materials and realizing their full potential in high-efficiency plasmonics-based optoelectronic devices, photovoltaics, biomedical and gas sensing applications [21-25].

2. Experimental procedure

The SnO_2: Au thin films were prepared on glass substrates using a DC sputtering system as illustrated in (Figure 1) which is equipped with a custom built substrate holder that is designed to implement the GLancing Angle Deposition (GLAD) technique. Prior to deposition, the glass substrates underwent a thorough cleaning process, followed by drying with nitrogen gas. The gold-doped tin dioxide thin films were deposited through co-sputtering where gold was incorporated in-situ during the growth of SnO_2 resulting in a doped system, Au has been prepared with a constant deposition angle of 80°. Then, an annealing has been performed. High purity Sn (99.99%) and Au (99.99%) targets were employed in the process. The films were deposited at four different incidence angles for the particle flux: 0° (normal deposition) as displayed in Figure 2(a), 40°, 60° and 80° in Figure 2(b). The sputtering parameters include a constant current density of 50 A/m², a magnetic field of 600 Gauss, and a base pressure of approximately 10^{-5} Pa, and they were carefully maintained to ensure process consistency.

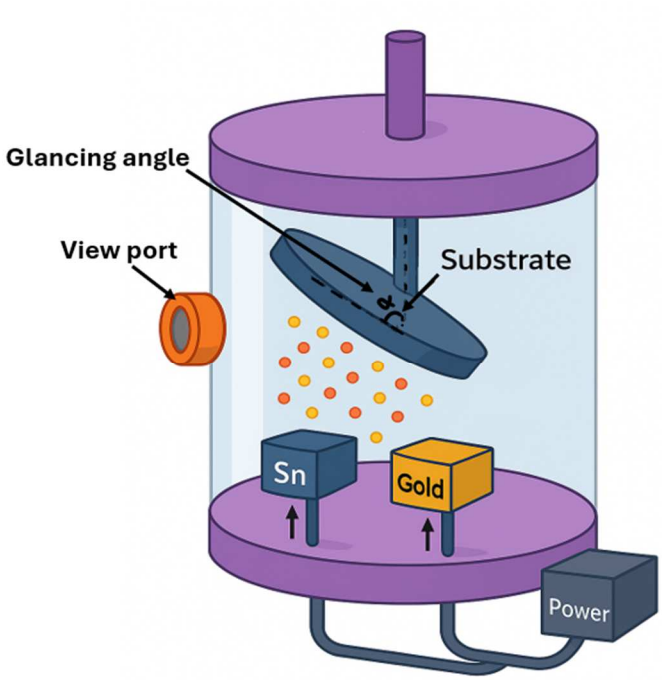

Figure.1: Schematic illustration of a DC sputtering device.

Figure 2(b) visually depicts the characteristic columnar growth structure achieved by the oblique angle deposition using the GLancing Angle Deposition (GLAD) technique. As observed, the schematic illustrates a film comprising inclined columns growing on a glass substrate, with their inclination directly correlating to the 80° oblique angle of the incident particle flux during deposition. This columnar morphology arises from the self-shadowing effect, where previously deposited material preferentially guides growth in the direction of the incoming flux. To comprehensively understand the films' structural and optical behavior, the deposited SnO_2:Au thin films went through attentive assessment. X-ray diffraction (XRD), performed with an ARL Equinox 300 diffractometer, was employed to identify crystalline phases (SnO_2 and surface deposited gold), preferred orientations, and crystallite sizes. Complementing this, optical transmittance measurements were conducted across a wide wavelength range using a UV-Visible spectrophotometer. These measurements were important for determining the film's transparency, absorption characteristics, and the influence of plasmonic effects from the incorporated gold, thereby clarifying how deposition parameters, such as the GLancing angle, affect light interaction and optimize performance for optoelectronic applications

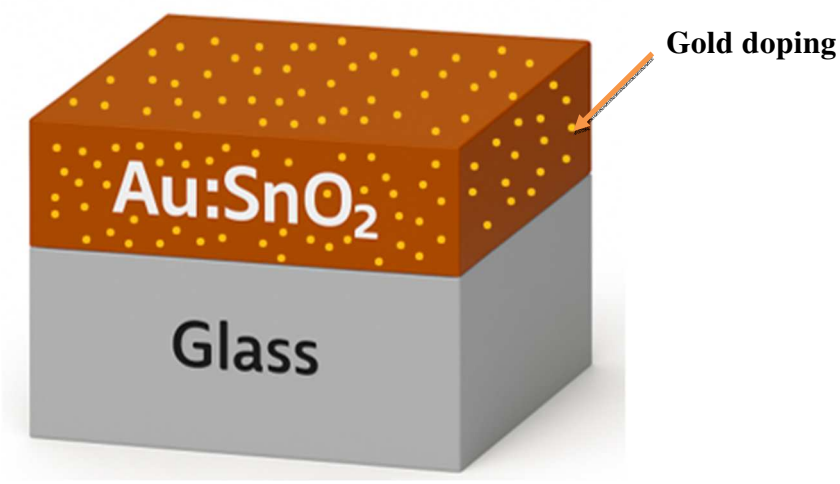

(a)

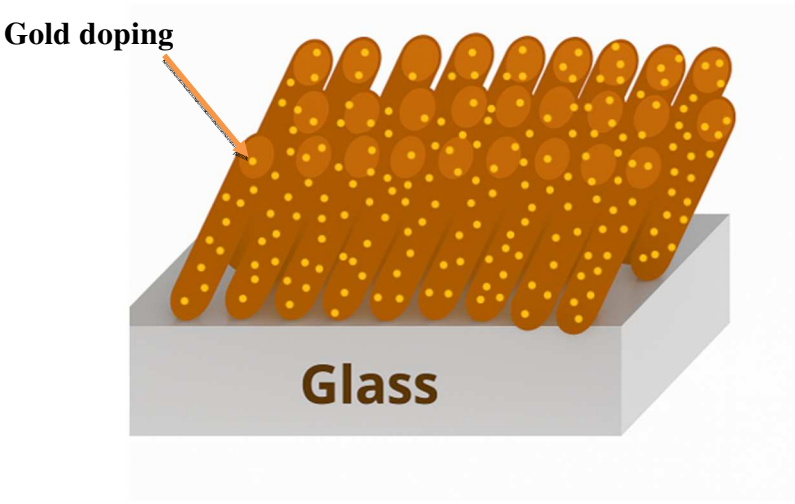

(b)

Figure.2: Schematic of (a) SnO_2:Au deposited at α= 0° and (b) SnO_2:Au deposited at α= 80°.

3. Results and discussion

Figure 3(b) displays the optical transmittance of the Gold-doped tin dioxide thin films, deposited at angles of α=0°, 40°, 60°, and 80°, as measured by UV-Visible spectrophotometry. A very distinct and progressive difference in optical transparency is observed, the film deposited at a planar angle (α=0°) exhibits the highest transmittance across the visible and near-infrared spectral range and as the deposition angle increases, the transmittance decreases. For instance, at a wavelength of around 550 nm, the planar sample shows a transmittance of approximately 48%, while the samples deposited at 40°, 60°, and 80° show progressively increased transmittances of approximately 45%, 42%, and 30%, respectively. This pattern is consistent with general observations for nanostructured films and noble metal inclusions. The decreased transparency of the oblique samples is a strong indicator of the significant morphological changes and optical effects caused by the GLAD technique and the presence of doped gold. Oblique deposition leads to the formation of inclined columnar structures and increased void fractions within the SnO_2 matrix, with these effects becoming more pronounced at higher angles. This nanostructuring creates a rougher and more porous film. The incorporated gold, especially if forming nanoparticles or clusters

within this porous SnO_2 matrix, strongly interact with incident light through localized surface plasmon resonance (LSPR). The LSPR phenomenon leads to enhanced light absorption and scattering at specific wavelengths, which directly contributes to the observed reduction in transmittance.

To further analyse this behaviour, we turn to the optical absorbance spectra shown in Figure 3(a) where the absorbance spectra reveal characteristic broad absorption peaks for all samples in the visible region. An interesting observation is the shift in the LSPR peak position and a progressive increase in its intensity as the deposition angle increases. The planar film (α=0°) shows an LSPR peak centred around 550 nm. As the deposition angle increases, the peak red-shifts, with the samples at 40° and 60° showing peaks around 600-650 nm, and the sample at 80° showing a peak centred at approximately 650-700 nm. This red-shift is likely due to the change in morphology of the gold nanoparticles, which become more elongated or form larger clusters at higher deposition angles, thus absorbing and scattering light at longer wavelengths. The film deposited at α=80° exhibits the most enhanced absorbance around its LSPR peak, while the planar film (α=0°) shows a lower overall absorbance with a peak at a shorter wavelength, consistent with the observed transparency patterns.

The SnO_2:Au thin films exhibit a direct optical band gap where the values for films deposited at angles of 0°, 40°, 60°, and 80° are found to be within the range of 3.88 eV to 3.95 eV. This narrow variation shows that the optical band gap remains relatively stable and is largely unaffected by the varying deposition angle. While the GLAD technique significantly influences the films' morphology and light scattering properties, its impact on the fundamental electronic band structure is minimal, with the observed blue-shift relative to bulk SnO_2 being consistent with the effects of quantum confinement and doping.

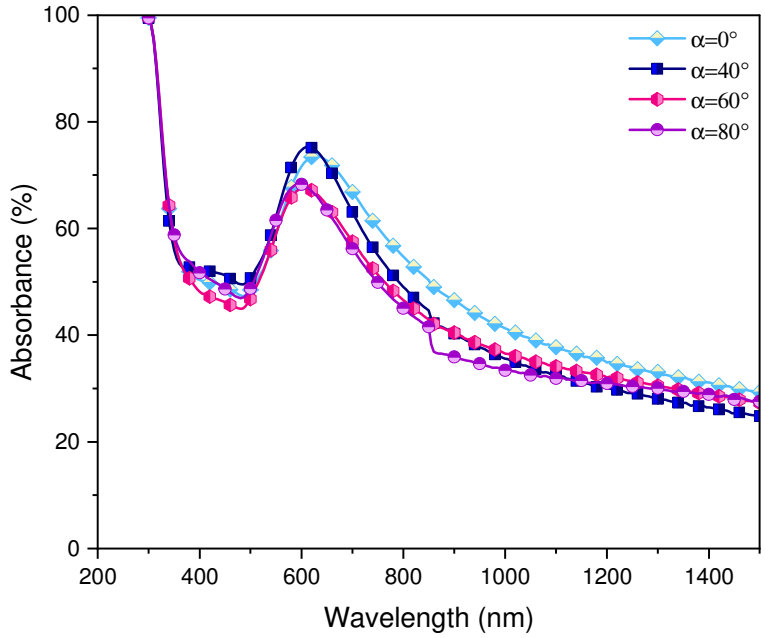

(a)

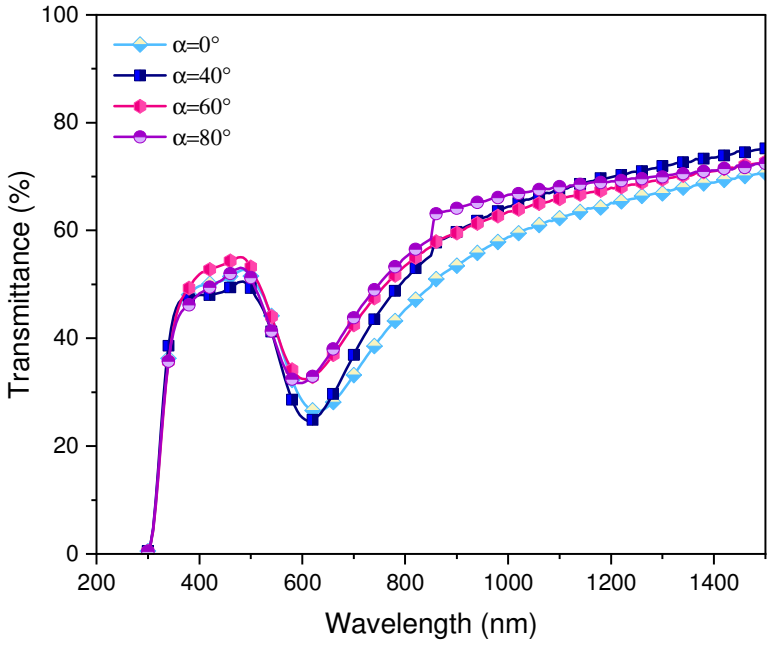

(b)

Figure. 3: Absorbance (a) and Transmittance (b) spectra of SnO_2:Au thin films deposited at α=0°, 40°, 60° and 80°.

The decreased transparency of the oblique samples can be directly attributed to morphological and optical effects induced by the GLAD process and the incorporation of gold. To confirm this correlation, additional SEM analyses, including surface and cross-sectional imaging, were performed for the Au-doped SnO_2 thin films deposited at different angles (0° and 80°). The newly added SEM micrographs (Figure 4(a–d)) clearly reveal the evolution of the film morphology with increasing deposition angle. The planar film (0°) exhibits a dense and compact structure, indicative of classical growth, while films deposited at oblique angles display inclined columnar features and a progressively increased porosity and surface roughness, directly confirming the GLAD-induced nanostructuring. Moreover, a granular and poorly columnar architecture is observed for the films prepared under normal incidence, corresponding to conventional dense growth. As the deposition angle increases, the shadowing effect becomes dominant, particularly for angles higher than 70°, leading to the formation of tilted columns aligned with the direction of the incoming particle flux. Consequently, the films deposited at high angles exhibit a more voided structure with significant spaces between the inclined columns. From the surface observations, Au nanoparticles, mostly egg-shaped and ranging from 50 to 200 nm, are distinctly visible. These nanoparticles are uniformly distributed on the SnO_2 surface and appear denser for the highest deposition angles. These new results provide direct experimental evidence supporting the earlier assumptions regarding the morphology and substantiate the correlation between the structural evolution and the observed optical behavior, specifically, the reduced transmittance and red-shifted LSPR peaks with increasing deposition angle. The inclusion of SEM data has therefore significantly strengthened the discussion and validated the role of both the GLAD technique and gold incorporation in tailoring the nanostructure and optical response of SnO_2 thin films.

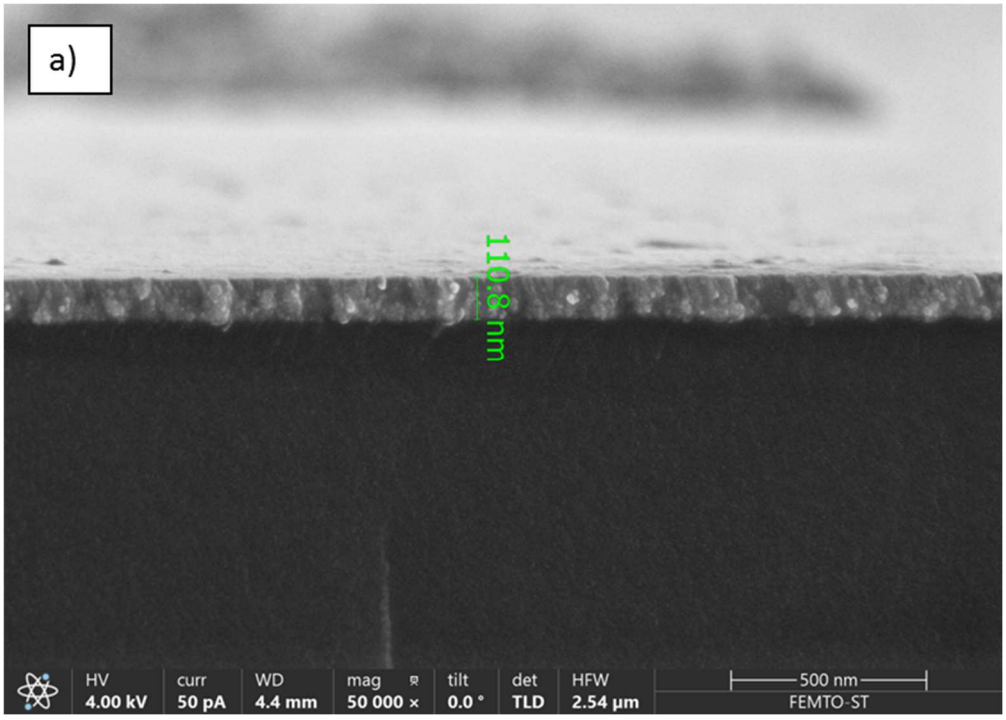
a)
110.8 nm
HV
4.00 kV
curr
50 pA
WD
4.4 mm
mag
50 000 ×
tilt
0.0 °
det
TLD
HFW
2.54 µm
500 nm
FEMTO-ST

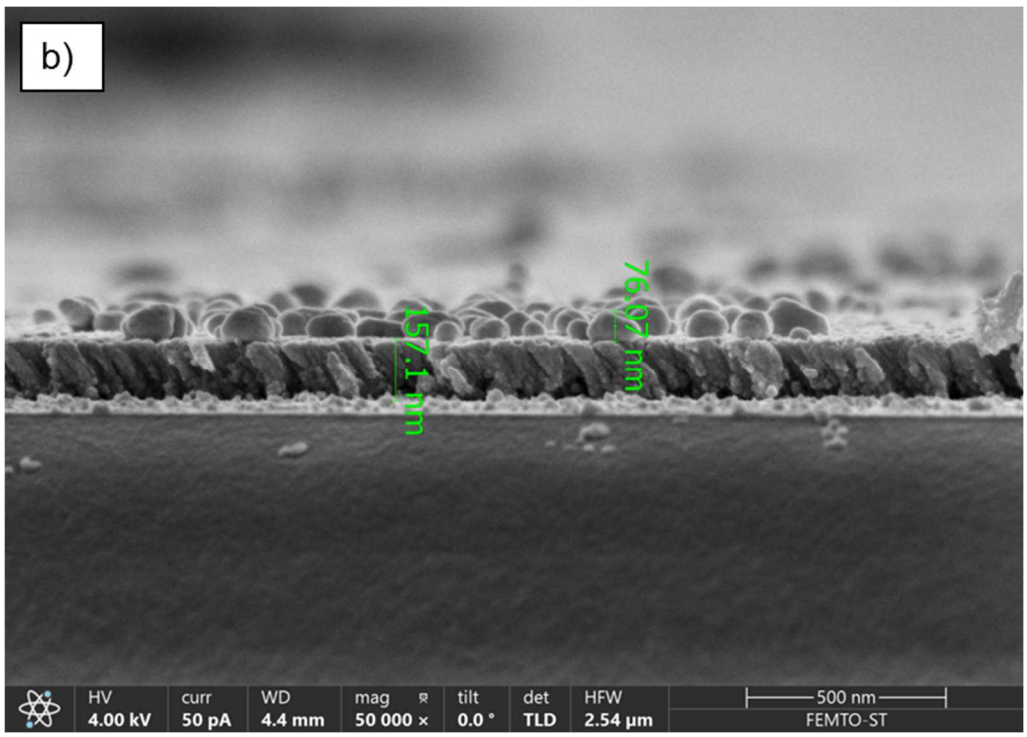
b)
76.07 nm
157.1 nm
HV
4.00 kV
curr
50 pA
WD
4.4 mm
mag
50 000 ×
tilt
0.0 °
det
TLD
HFW
2.54 µm
500 nm
FEMTO-ST

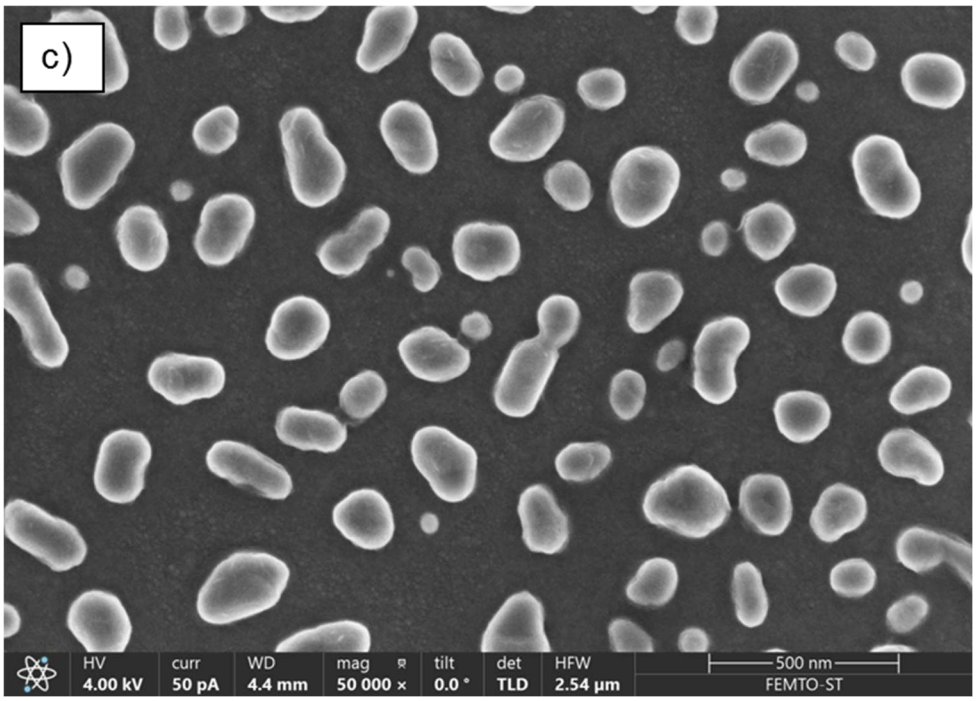

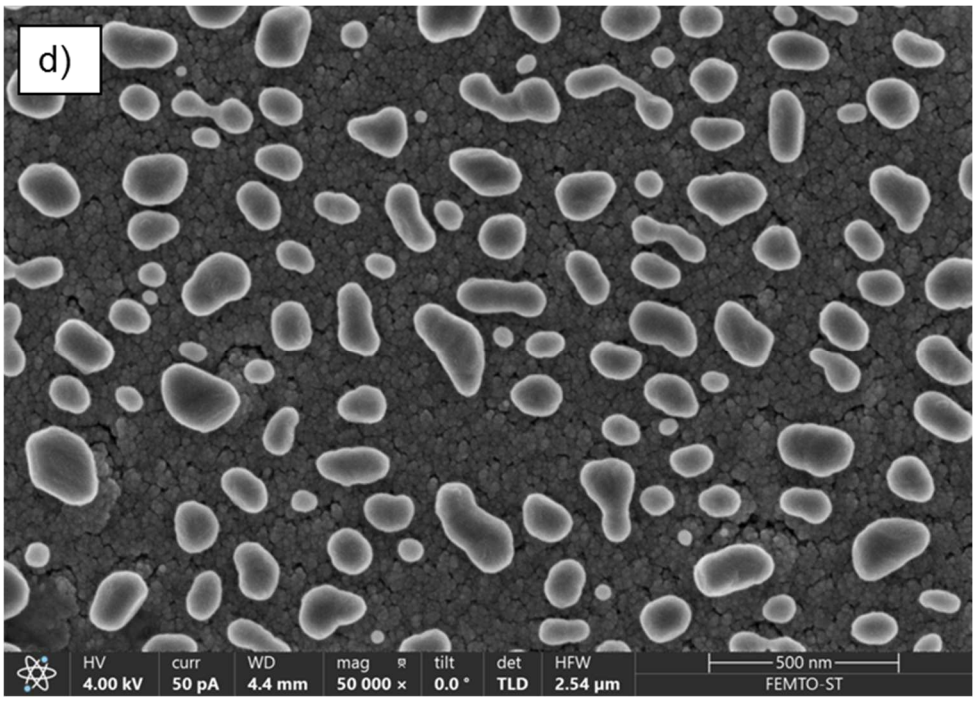

Figure. 4: Cross section and top views of SnO_2:Au thin films prepared with a deposition angle $\alpha = 0°$ (3a and 3c) and $\alpha = 80°$ (3b and 3d).

The X-ray diffraction (XRD) patterns of the SnO_2: Au thin films, as observed in Figure 5(a) and (b), provide an insight into the crystalline structure and phase composition of the SnO_2:Au thin films, fabricated at various deposition angles. The patterns, observed for all four angles (0°, 40°, 60°, and 80°), consistently confirm a well-defined polycrystalline nature. The host matrix is definitively identified as tetragonal rutile SnO_2, which is evidenced by the presence of multiple, distinct diffraction peaks. These include the (101) peak at approximately 34°, and others corresponding to the (100) and (211) planes. The sharp, consistent appearance of these peaks across all samples confirms that the crystalline structure of the SnO_2 host remains stable and robust despite the gold incorporation and the significant differences in growth conditions imposed by the GLAD technique. Crucially, the successful integration of gold is confirmed by a separate set of well-defined peaks. These belong to the face-centered cubic (FCC) structure of metallic gold, with the most prominent peak corresponding to the (111) plane at about 38.1°. Other gold peaks, such as the (200), (220), (311), and (222) planes, are also present, which shows clearly that the gold exists as a separate phase of very small crystals within the films. This observation confirms that gold does not form a solid solution with SnO_2, but rather nucleates and grows as discrete nanoparticles, which is the prerequisite for the observed localized surface plasmon resonance (LSPR) effect. While the phase composition is consistent, a detailed comparison across the samples reveals subtle yet significant effects of the deposition angle on the film's microstructure. Planar deposition (α=0°) is a more uniform process, whereas the oblique angles (40°, 60°, 80°) introduce kinetic limitations through the atomic shadowing effect. As the angle increases, the limited surface adatom mobility leads to the formation of increasingly porous films with inclined columnar structures. These morphological changes are reflected in the XRD patterns. For instance, the columnar growth can induce a preferred orientation, or texture, where certain crystallographic planes preferentially align leading to changes in the relative intensities of the diffraction

peaks. Furthermore, the limited surface atom diffusion can result in the formation of smaller crystallites, which would manifest as a broadening of the diffraction peaks, consistent with the principle that smaller crystallites produce wider peaks. Similarly, the unique growth environment affects the nucleation and size distribution of the embedded gold nanoparticles, which can alter the sharpness and intensity of their corresponding diffraction peaks, and it is also observed that a larger amount of gold is incorporated in the oblique films.

Crucially, the successful incorporation of gold is confirmed by distinct peaks corresponding to the face-centered cubic (FCC) structure of metallic Au, with the most intense reflection from the (111) plane at about 38.1°. Other gold-related peaks ((200), (220), and (311)) are also visible, confirming the presence of well-dispersed Au nanocrystals within the SnO_2 matrix. While all films exhibit a stable tetragonal rutile SnO_2 structure, a noticeable dependence of the diffraction peak width and intensity on the deposition angle is observed. To quantitatively assess this effect, the average crystallite size (D) of the SnO_2 phase was calculated using the Scherrer equation:

$$D = (K\lambda) / (\beta \cos\theta) \quad (1)$$

where $K = 0.9$, $\lambda = 1.5406$ Å (Cu Kα), β is the full width at half maximum (FWHM), and θ is the Bragg angle. The estimated crystallite sizes are 24.6 nm (0°), 21.8 nm (40°), 19.3 nm (60°), and 16.7 nm (80°), indicating a clear reduction in crystallite size with increasing deposition angle. This trend is consistent with the enhanced atomic shadowing and limited surface diffusion occurring under oblique flux incidence during GLAD, which promotes the formation of finer grains and columnar structures. The observed broadening of the SnO_2 diffraction peaks and the reduction in crystallite size are therefore consistent with the morphological evolution confirmed by SEM imaging.

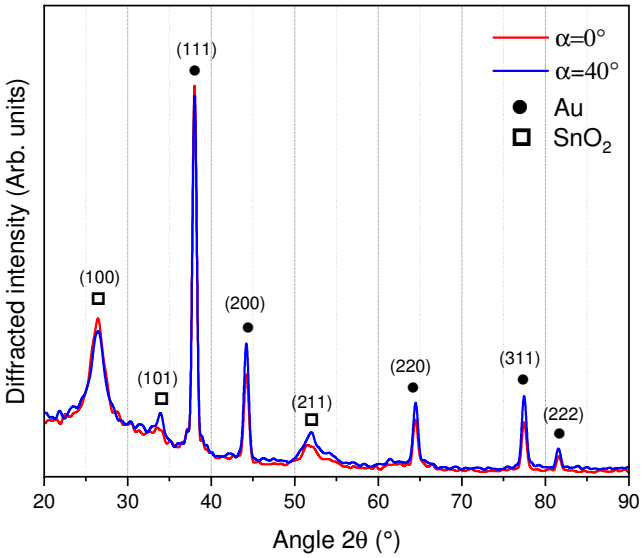

(a)

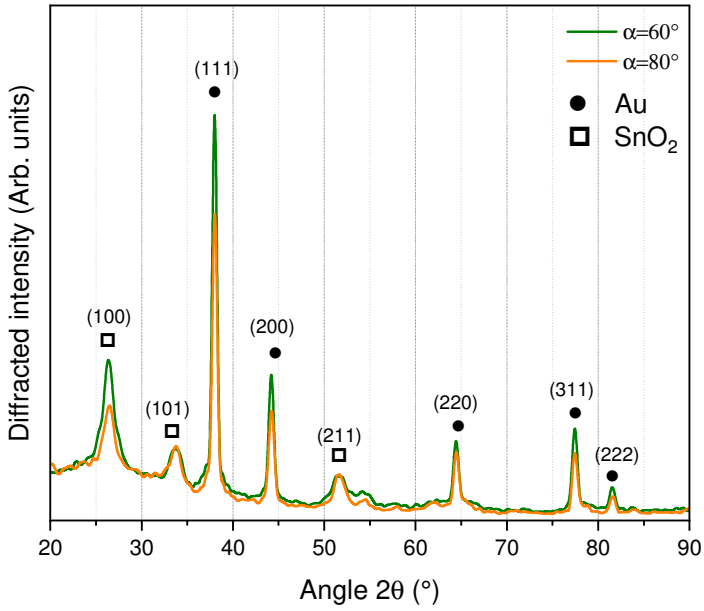

(b)

Figure.5: Structural properties via XRD of SnO_2: Au thin films deposited at (a) α=0° and 40° & (b) α=60° and 80°.

The plots of LSPR peak position and optical band gap as a function of deposition angle in Figure 6 (a) and (b) reveal extremely interesting insights into the influence of GLAD. The LSPR peak position exhibits a clear red-shift as mentioned previously, moving to longer wavelengths (from ~550 nm to ~680 nm) as the deposition angle increases. This confirms that the oblique deposition significantly influences the size, shape, and aggregation of the gold nanoparticles, leading to tunable plasmonic resonance. In contrast, the optical band gap of the SnO_2: Au films remains remarkably stable, showing only minimal variation (from 3.88 eV to 3.95 eV) across all deposition angles. This stability would most likely indicate that while GLAD profoundly modifies the film's morphology and thereby its light scattering and plasmonic response, it does not significantly alter the fundamental electronic band structure of the SnO_2 host matrix. The plots of LSPR peak position and optical band gap as a function of deposition angle (Figure 6(a) and (b)) provide important insight into the influence of GLAD on the optical response of the Au-doped SnO_2 thin films. The LSPR peak exhibits a pronounced red-shift, moving from approximately 550 nm for the planar film to about 680 nm for the sample deposited at 80°. While this shift can be attributed in part to the growth and aggregation of Au nanoparticles at higher deposition angles, other contributing factors must also be considered. In particular, the increased porosity and variation in the dielectric environment of the SnO_2 host, both induced by oblique deposition, can modify the local refractive index surrounding the nanoparticles and thereby alter their plasmonic resonance conditions. This combined effect of nanoparticle morphology, porosity, and dielectric modulation provides a more comprehensive explanation of the tunable plasmonic behavior observed in the GLAD-deposited films. The optical band gap (E_g) was determined from the absorption spectra using Tauc plots of $(\alpha h\nu)^2$ versus photon energy ($h\nu$), assuming a direct allowed transition. The extrapolation of the linear portion of the plot to $(\alpha h\nu)^2 = 0$ yields the optical band gap value. Fitting was performed over the most linear region of the curves,

resulting in an estimated uncertainty of ±0.03 eV. The extracted band gap values (3.88–3.95 eV) exhibit only a minor variation with deposition angle, which falls within the experimental error margin and indicates that the fundamental electronic structure of SnO_2 remains largely unaffected by GLAD. However, the slight increase in E_g at higher angles could arise from subtle changes in film density, increased surface roughness, or minor variations in defect states and oxygen vacancies, which can slightly modify the optical absorption edge. Overall, the results confirm that the GLAD process significantly alters the plasmonic response through morphological and dielectric modulation, while maintaining stable electronic properties of the Au-doped SnO_2 matrix.

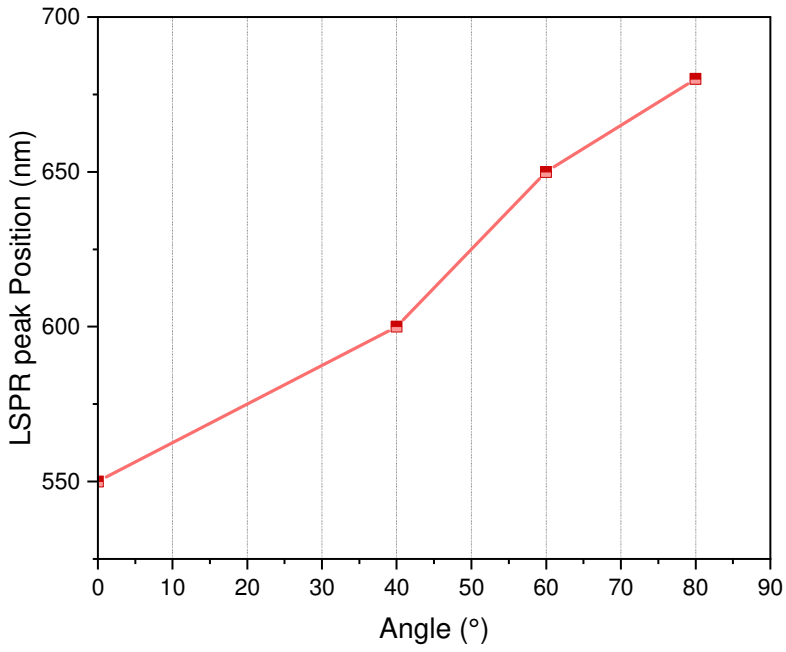

(a)

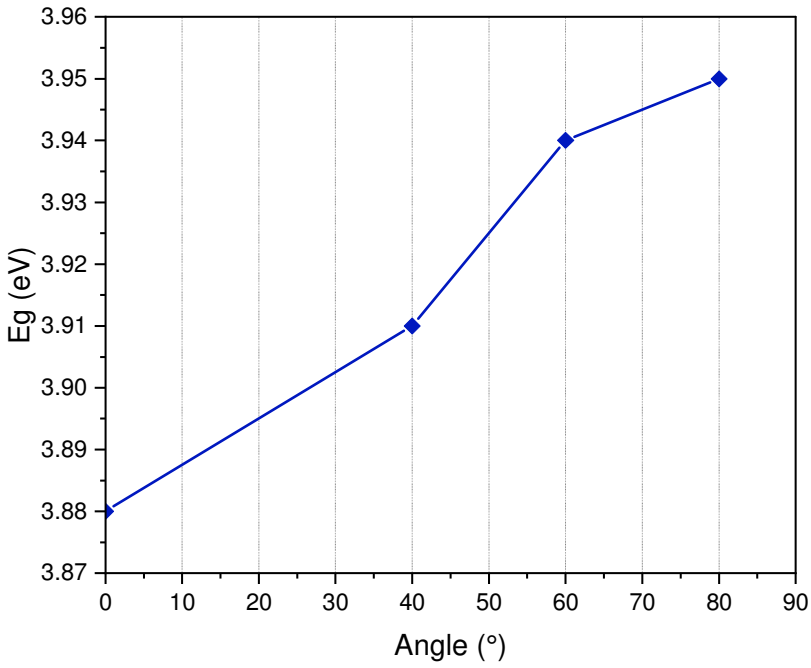

(b)

Figure.6: (a) LSPR peak position depending on the GLancing angle for SnO_2: Au thin films, (b) Impact of the GLancing angle on the band gap (Eg) of SnO_2: Au thin films.

Based on our findings, it is observed how much the deposition angle affects the optical properties of the gold doped tin dioxide thin films. Table 1 presents a comprehensive comparative analysis of the optical properties of these films, emphasizing the transparency changes. At a wavelength of approximately 550 nm, the optical transparency displays a clear and progressive decrease as the deposition angle increases, dropping from 48% for the planar film (α=0°) to a substantially reduced 30% for the highly oblique film (α=80°). This significant reduction in transparency is a strong indicator of a remarkable change in the way light interacts with the films. The optical absorbance at the same wavelength shows a different pattern, despite the fact that this drop in transparency might indicate a straightforward increase in absorption. Absorbance at 550 nm shows a slight decrease as the films become more oblique, dropping from approximately 50% for the planar film to about 42% for the film deposited at 80°. This result, when considered alongside the full absorption spectra, means

that the dominant mechanism for the reduced transparency in the oblique films is enhanced light scattering by the nanostructured, porous morphology induced by the GLancing Angle Deposition (GLAD) technique, rather than solely increased absorption. Besides that, the presence of gold nanoparticles introduces another interesting layer of control. As the films become more oblique, we observe a significant red-shift in the localized surface plasmon resonance (LSPR) peak, shifting it from approximately 550 nm to about 680 nm. This change is a direct result of the altered nanostructure, which modulates the plasmonic behaviour and enables the films to interact with light at longer wavelengths. Furthermore, the optical band gap shows a slight, progressive increase with deposition angle, rising from 3.88 eV for the planar film to 3.95 eV for the most oblique film. Although this change is pretty minor, it proposes that the GLAD-induced morphological changes slightly influence the film's effective electronic structure.

Table.1: Optical properties of SnO_2: Au thin films deposited at different angles (0°, 40°, 60° and 80°).

Deposition angle	**(α=0°)**	**(α=40°)**	**(α=60°)**	**(α=80°)**
Optical transparency ~550 nm (%)	48%	45%	42%	30%
Optical absorbance ~550 nm (%)	~50%	~48%	~47%	~42%
Band gap (eV)	3.88	3.91	3.94	3.95
LSPR peak position	~550	~600	~650	~680

4. Conclusion

This study has successfully synthesized Au-doped SnO_2 thin films via DC sputtering and GLancing Angle Deposition (GLAD) across angles of 0°, 40°, 60°, and 80°. XRD analysis confirmed the polycrystalline nature of the SnO_2 matrix and the effective incorporation of metallic gold nanocrystallites, with GLAD influencing the film's microstructure. Complementary SEM surface and cross-sectional analyses further revealed the morphological evolution induced by oblique deposition, showing a transition from dense and compact structures at normal incidence to highly porous and columnar architectures at larger

deposition angles. The formation of inclined columns and increased surface roughness confirmed the GLAD-induced nanostructuring and provided direct evidence linking morphology to the optical properties. Optically, a significant and progressive decrease in transparency was observed with increasing deposition angle (from 48% to 30% at 550 nm), primarily due to enhanced light scattering from the GLAD-induced nanostructured morphology and increased porosity. Simultaneously, the localized surface plasmon resonance (LSPR) peak, attributed to the gold nanoparticles, exhibited a distinct red-shift (from ~550 nm to ~680 nm) with increasing angle, demonstrating tunable and modulation of the plasmonic properties. Notably, despite these substantial morphological and plasmonic changes, the optical band gap of the films remained remarkably stable (ranging from 3.88 eV to 3.95 eV). Overall, the combination of GLAD and noble metal doping offers a powerful and versatile strategy for precisely tailoring the structural and optical properties of Au-doped SnO_2 films for a wide range of optoelectronic applications, including photodetectors, solar cells, and gas, chemical, and biological sensors. Furthermore, the proposed experimental approach can be extended by exploring the effects of large GLancing angles and deposition power values to assess their influence on the LSPR peaks and the resulting optoelectronic properties.

References

[1] L. Li and Z. Fan, “Optoelectronic Materials and Devices,” Small Methods, vol. 8, no. 2, Feb. 2024.

[2] P. K. Nayak, S. Mahesh, H. J. Snaith, and D. Cahen, "Photovoltaic solar cell technologies: analysing the state of the art," Nat Rev Mater, vol. 4, pp. 269–285, 2019.

[3] E. Fortunato, D. Ginley, H. Hosono, D.C. Paine, "Transparent conducting oxides for photovoltaics," MRS bulletin, vol. 32, pp. 242-247, 2007.

[4] A.Cruz, et al., "Effect of front TCO on the performance of rear-junction silicon heterojunction solar cells: Insights from simulations and experiments," Solar Energy Materials and Solar Cells, vol.195, pp.339-345, 2019.

[5] A. Kocyigit and G. Kerimli, “The characterization of various TCOs and metal oxide layers for dye sensitized solar cells,” Mater Today Proc, vol. 46, pp. 6947–6953, 2021.

[6] H. Ferhati and F. Djeffal, “Performance assessment of TCO/metal/TCO multilayer transparent electrodes: from design concept to optimization,” J Comput Electron, vol. 19, pp. 815–824, 2020.

[7] D. Y. Kang et al., “Dopant-Tunable Ultrathin Transparent Conductive Oxides for Efficient Energy Conversion Devices.,” Nanomicro Lett, vol. 13, p. 211, 2021.

[8] F. Djeffal, H. Ferhati, A. Benyahia, and Z. Dibi, “Performance analysis of SnS photodetector using strained SnO2 stacked layer: Numerical simulation and DFT calculations,” Microelectron Eng, vol. 273, p. 111961, Mar. 2023.

[9] D. Rechem., A. Khial., A. Souifi, F. Djeffal, “Effect of annealing time on the performance of tin oxide thin films ultraviolet photodetectors,” Thin Solid Films, vol. 623, pp. 1-7, 2017.

[10] H. Ferhati, F. Djeffal, A. Bendjerad, A. Benhaya, A. Saidi, “Perovskite/InGaAs tandem cell exceeding 29% efficiency via optimizing spectral splitter based on RF sputtered ITO/Ag/ITO ultra-thin structure,” Physica E: Low-dimensional Systems and Nanostructures, vol. 128, pp. 114618, 2021.

[11] G. Kiruthiga, K. S. Rajni, N. Geethanjali, T. Raguram, E. Nandhakumar, and N. Senthilkumar, “SnO_2: Investigation of optical, structural, and electrical properties of transparent conductive oxide thin films prepared by nebulized spray pyrolysis for photovoltaic applications,” Inorg Chem Commun, vol. 145, pp. 109968, 2022.

[12] H. Ferhati, F. Djeffal, and F. AbdelMalek, “Towards improved efficiency of SnS solar cells using back grooves and strained-SnO2 buffer layer: FDTD and DFT calculations,” Journal of Physics and Chemistry of Solids, vol. 178, p. 111353, 2023.

[13] S. Pramanik et al., “Role of plasmonic layer with SnO2 thin film to improve UV photoluminescence and photoresponse,” Surfaces and Interfaces, vol. 51, pp. 104617. 2024.

[14] N. Zhang et al., “Synthesis of au-decorated SnO_2 crystallites with exposed (221) facets and their enhanced acetylene sensing properties,” Sens Actuators B Chem, vol. 307, p. 127629, 2020.

[15] E. Ovodok, V. Kormosh, V. Bilanych, and M. Ivanovskaya, “Semiconductor Metal Oxides Doped with Gold Nanoparticles for Use in Acetone Gas Sensors,” Journal of physics, vol. 2315, pp. 012018–012018, 2022.

[16] J. A. Schuller, E. S. Barnard, W. Cai, Y. C. Jun, J. S. White, and M. L. Brongersma, “Plasmonics for extreme light concentration and manipulation,” Nat Mater, vol. 9, pp. 193–204, 2010.

[17] H. A. Atwater and A. Polman, “Plasmonics for improved photovoltaic devices,” Nat Mater, vol. 9, pp. 205–213, 2010.

[18] A. El Mohajir et al., “Nanostructuring of SnO_2 Thin Films by Associating GLancing Angle Deposition and Sputtering Pressure for Gas Sensing Applications,” Chemosensors, vol. 10, pp. 426, 2022.

[19] H. Ferhati, F. Djeffal, and N. Martin, “Highly improved responsivity of self-powered UV–Visible photodetector based on TiO2/Ag/TiO2 multilayer deposited by GLAD technique: Effects of oriented columns and nano-sculptured surface,” Appl Surf Sci, vol. 529, p. 147069, 2020.

[20] H. Ferhati, F. Djeffal, N. Martin, and A. Benhaya, “Tunable properties of SnOx sputter-deposited by RGPP and GLAD techniques: A potential candidate for photosensing and all-oxide solar cells,” Solar Energy, vol. 268, p. 112305, 2024.

[21] M. Mezyen, N. Bitri, I. Riahi, F. Chaabouni, and E. Llobet, “Optimizing Sputtered SnO2:Dy Thin Films for NO2 Gas Detection,” Chemosensors, vol. 13, pp. 121, 2025.

[22] K. A. Willets and R. P. Van Duyne, “Localized surface plasmon resonance spectroscopy and sensing,” Annu Rev Phys Chem, vol. 58, pp. 267–297, 2007.

[23] T. Ohgaki et al., “Synthesizing SnO_2 thin films and characterizing sensing performances,” Sens Actuators B Chem, vol. 150, pp. 99–104, 2010.

[24] H. Ferhati, N. Martin, F. Djeffal, “ Boosting the Efficiency of SnS Solar Cells Through Reactively Sputter-Deposited Ag-Nanostructured Layer/SnO2 Film at GLancing Angles,”. Plasmonics, vol. 20, pp. 741–752, 2025.

[25] H. Ferhati, T. Berghout, F. Djeffal, “Efficient SnS solar cells via plasmonic light trapping and alternative buffer layers: a combined machine learning and FDTD analysis,” Plasmonics, vol. 20, pp. 253-263, 2025.